Histol Histopathol (2023) 38: 233-245

http://www.hh.um.es

Histology and Histopathology
From Cell Biology to Tissue Engineering

ORIGINAL ARTICLE **Open Access**

Albiflorin relieves cerebral ischemia-reperfusion injury by activating Nrf2/HO-1 pathway

Fei Zhu[1], Jianzhong Xiong[2], Fei Yi[1], Ermin Luo[1], Chun Huang[1] and Runying Li[3]

[1]Department of Neurology, [2]Department of Rehabilitation and

[3]Department of Stomatology, Pingxiang People's Hospital, Jiangxi Province, PR China

Summary. Our work aims to investigate the functions of a natural compound, Albiflorin (AF) in cerebral ischemia-reperfusion (IR) injury. The cerebral IR models were established by OGD/R in PC12 cells and MCAO/IR in rats. The cells in a glucose-free medium were placed in an anaerobic chamber containing 95% N_2 and 5% CO_2 for 3h at 37°C, returned to a normal medium, and incubated for 24h to accomplish OGD/R. Focal cerebral ischemia was conducted by thread occlusion of the right middle cerebral artery for 2h followed by 24h reperfusion in rats. CCK-8 assay indicated that AF had no toxicity to PC12 cells. Flow cytometry, Western blot, or TUNEL showed that AF treatment reduced apoptosis of cells or rat brain tissues. qRT-PCR and ELISA showed that AF decreased IL-1β, IL-6, and TNF-α levels *in vitro* and *in vivo*. Elevated levels of MDA, SOD, and ROS induced by IR injury were mitigated by AF *in vitro* and *in vivo*. HE and TTC staining revealed that AF ameliorated pathological injury in MCAO/IR rats. Western blot showed that Nrf2, NQO1, and HO-1 expression was activated by AF, and ML385 treatment suppressed the inhibition effects of AF in cerebral IR injury models. Overall, AF alleviates cerebral IR injury via regulating the Nrf2/HO-1 pathway.

Key words: Albiflorin, Cerebral ischemia-reperfusion, Nrf2/HO-1, Apoptosis, Inflammation, Oxidative stress

Introduction

Ischemic cerebrovascular disease can bring about neurological dysfunction of varying degrees and is considered a serious threat to the public due to the high morbidity, disability rate, and mortality rate (Cai et al., 2021). Cerebral ischemia-reperfusion (IR) injury refers to the sudden resumption of blood supply to the brain after permanent or transient ischemia (Block et al., 2020). However, the brain function is not only failed to recover after reperfusion, but more severe neuronal dysfunction will also occur Therefore, reducing cerebral IR injury is the key problem to be solved urgently in the treatment of ischemic cerebrovascular disease.

Cerebral IR injury involves various pathophysiological processes, such as oxidative stress, neuronal apoptosis, and inflammatory response (Naderi et al., 2020). Activation of inflammatory cells and elevated production of proinflammatory factors, accompanied by oxidative stress and free radical production, lead to neuronal apoptosis, axonal degeneration, synaptic plasticity, and transmission disorders (Bramlett and Dietrich, 2004). Evidence showed that inflammatory cytokines overexpression and inflammatory cell infiltration occurred after cerebral IR, leading to a series of inflammatory responses (Wu et al., 2020). Oxidative stress is involved in inflammatory responses and neuronal apoptosis and is also a consequence of cerebral IR damage, which in turn exacerbates injury (Ikeda et al., 2013). Nuclear factor-E2-related factor 2 (Nrf2) is an endogenous factor in brain tissues and a transcription factor of the leucine zipper family, it exerts a vital role in alleviating oxidative stress and inflammatory response (Wang et al., 2011). In recent years, Nrf2 activation has been shown to alleviate oxidative damage caused by cerebral IR, and enzyme heme oxygenase 1 (HO-1) deficient mice

Corresponding Author: Jyh-Yih Chen, Runying Li, No. 8, Wugongshan middle Avenue, Pingxiang Development Zone, Jiangxi Province, PR China. e-mail: lirunyinglry@163.com

DOI: 10.14670/HH-18-518

Abbreviations. OGD/R, oxygen-glucose deprivation/reperfusion; MCAO/IR, middle cerebral artery occlusion/ischemic-reperfusion; CCK-8, cell counting kit-8; TUNEL, terminal deoxynucleotidyl transferase-mediated dUTP nick-end labeling; qRT-PCR, quantitative Real-Time PCR; ELISA, enzyme-linked immunosorbent assay; HE, hematoxylin and eosin; IL-1β, interleukin-1β; IL-6, interleukin-6; TNF-α, tumor necrosis factor-α; MDA, malondialdehyde; SOD, superoxide dismutase; ROS, reactive oxygen species; TTC, 2,3,5-Triphenyltetrazolium chloride; Nrf2, nuclear factor-E2-related factor 2; HO-1, enzyme heme oxygenase 1; NQO1, quinone oxidoreductase 1.

showed more serious brain damage (Ginet et al., 2009). Therefore, the Nrf2/HO-1 pathway might be regarded as an underlying target for neuroprotective treatment of cerebral IR injury.

Paeonia Alba Radix is the dried root of *P. lactiflora Pallas* or *P. veitchi*i *Lynch*. It has sorts of medicinal properties, including blood circulation and pain relief, and has been widely used for hundreds of years in traditional Chinese prescription (Ma et al., 2015; Zhu et al., 2015). Albiflorin (AF) is the main glycoside component in *P. alba Radix*. In clinical reports and preclinical studies, AF has been identified to have effective anti-inflammatory and anti-depressant activities (Song et al., 2015). Also, AF has been demonstrated to display apparent analgetic effects on neuropathic pain rats induced by peripheral nerve injury (Zhou et al., 2016). Moreover, studies have shown that AF exerted antioxidant effects (Ma et al., 2015). However, as far as we know, no research has examined the effect and mechanism of AF in cerebral IR injury. Based on the above evidence, we speculated that AF probably plays a role in alleviating cerebral IR injury and neuroprotection.

Therefore, this work examined the protective effect and underlying mechanism of AF in cerebral IR injury using PC12 cells and a rat model. We first found that AF alleviates cerebral IR injury *in vitro* and *in vivo* via activating Nrf2/HO-1 pathway. The present work provided a novel theoretical basis for further prevention and treatment of cerebral IR injury.

Materials and methods

Cell treatment

The PC12 cell line was commercially purchased from ATCC (USA) and cultured in Dulbecco's Modified Eagle Medium (DMEM, Thermo Fisher, USA) comprising 10% fetal bovine serum (Gibco, USA). Cells were cultivated in an incubator under 5% CO_2 and 37°C conditions. Before oxygen-glucose deprivation/reoxygenation (OGD/R) treatment, the medium was replaced by glucose-free DMEM. Cells were placed in an anaerobic chamber full of 95% N_2 and 5% CO_2 (v/v). Then, a normal medium was used to replace a glucose-free medium for 2 h to accomplish OGD/R stimulation. At last, the cells were put back into the incubator for further incubation for 24h. Cells cultured in a normal medium and under normoxic conditions served as control.

Cell viability assay

The PC12 cell viability was tested by cell counting kit-8 (CCK-8, Beyotime, China) assay. Cells were grown in 96-well plates (approximately 5000 cells in each well). CCK-8 reagent of 10 μL was supplied to each well and maintained for 1h at 37°C. Then, the results were read by a Microplate Reader (Bio-Rad, CA) at the absorbance of 450 nm.

Cell apoptosis assays

Annexin V-FITC/PI Detection Kit (Sangon Biotech, China) was used to detect cell apoptosis. Cells were seeded in 6-well plates (approximately $5x10^5$ cells per well). After stimulation, cells were washed using pre-cold phosphate buffer solution (PBS) 2 times and resuspended in 1xBinding buffer. Annexin V of 5 μL and PI of 5 μL were supplied to the suspension and incubated at 25°C in dark for 30 min. Flow cytometry (Beckman Coulter, USA) was used to detect apoptotic and necrotic cells. Data analysis was done using FlowJo software (Tree Star Inc., USA).

The apoptosis of rat brain tissues was measured by terminal deoxynucleotidyl transferase-mediated dUTP nick-end labeling (TUNEL, Roche, Sweitzerland) assay. Following the protocol, TUNEL staining was applied in frozen brain slices with 10 μm-thickness. Six rats in each group were randomly selected, and individual TUNEL positive cells were counted in the ischemic penumbra with a 1 mm^2 consecutive area. An observer, who was not informed of the study design, calculated the number of apoptotic cells per area in 20 consecutive visual fields in 4 sections of each rat. The average number of apoptotic cells in each visual field was calculated for each rat.

Enzyme-linked immunosorbent assay (ELISA)

The concentrations of interleukin-1β (IL-1β), interleukin-6 (IL-6), and tumor necrosis factor-α (TNF-α) in PC12 cells or rat brain tissues were tested by using the relevant ELISA kits (Abcam, China) following the corresponding protocol. The results were read by a Microplate Reader at 450 nm wavelength.

Oxidative stress detection

The level of intracellular reactive oxygen species (ROS) was detected using a fluorescence probe 2, 7-dichlorofluorescein diacetate kit (DCFH-DA, Sigma, China). In brief, cells seeded in 96-well plates were washed with PBS 3 times and incubated in DCFH-DA with the concentration of 10 mM at 37°C in dark for 30 min. After another three-time wash with PBS, the fluorescence images were acquired using a fluorescence microscope (Inova Diagnostics, USA) with 485 nm excitation wavelength and 520 nm emission wavelength.

The levels of (reactive oxygen) ROS, malondialdehyde (MDA), and superoxide dismutase (SOD) in PC12 cells and rat brain tissues were tested by relevant commercial assay kits (Abcam, China). In short, the cells or tissues were cracked and centrifuged at 12,000 g for 5 min at 4°C. The supernatant was collected and supplied with a working solution. After incubating for 30 min, the concentrations were acquired from a Microplate Reader at the absorbance of 450 nm.

Quantitative Real-Time PCR (qRT-PCR)

Total RNAs were isolated by using Trizol reagent (Thermo Fisher, USA) from PC12 cells. Primer Script RT reagent kit (Takara, Japan) was used to reversely transcribe RNA into cDNA. The mRNA expression of IL-1β, IL-6, and TNF-α was determined by an SYBR-Green qRT-PCR assay kit (Takara, Japan). GAPDH was used as a standardized control. The primers used in this part are as follows: IL-1β, forward: 5'-GAAATGCCACCTTTTGACAGTG-3' and reverse: 5'-TGGATGCTCTCATCAGGACAG-3'; IL-6, forward: 5'-TCCAGTTGCCTTCTTGGGAC-3' and reverse: 5'-AGACAGGTCTGTTGGGAGTG-3'; TNF-α, forward: 5'-AGCCGATGGGTTGTACCTTG-3' and reverse: 5'-ATAGCAAATCGGCTGACGGT-3'; GAPDH, forward: 5'-CACATGGCCTCCAAGGAGTAA-3' and reverse: 5'-TGAGGGTCTCTCTCTTCCTCTTGT-3'. Three replicates were set for each group to calculate the mean value of each experiment. Data were analyzed using $2^{-\triangle\triangle Ct}$ method.

Western blot

The Western blot was performed using hippocampal tissues from rat brains. the hippocampal samples were acquired from ischemic hemisphere portion and homogenized in RIPA lysis buffer (Beyotime, China). Cell proteins were prepared by using RIPA buffer containing protease inhibitors (Roche, Switzerland). The protein concentration was quantified by BCA Protein Assay Kit (Beyotime, China). The denatured protein of 20 μg was loaded, electrophoresed, and transferred to polyvinylidene fluoride (PVDF, Millipore, USA) membranes. Membranes were blocked with 5% milk at room temperature for 2 h and probed with primary antibodies (Cell signaling Technology, USA) overnight at 4°C. The primary antibodies were as follows: anti-cleaved caspase-3 (#9662, 1:1000), anti-Bax (#5023, 1:1000), anti-bcl-2 (#4223, 1:1000), anti-Nrf-2 (#12721, 1:1000), anti-Lamin B1 (#17416, 1:1000), anti-HO-1 (#86806, 1:1000), anti-NQO1 (#3187, 1:1000), and anti-β-actin (#4970, 1:2000). Next, the membranes were incubated with corresponding HRP-conjugated secondary antibodies (1:5000, Sigma, China) for 1.5 h at indoor temperature. The results were visualized by using an ECL reagent (Beyotime, China) to develop signals.

Middle cerebral artery occlusion/ischemic reperfusion (MCAO/IR)

The male Sprague Dawley (SD) rats (8 weeks; 280-320 g; Shanghai Alac Laboratory Animal Co., Ltd., China; 12 h light/dark cycle; total of 78) were subject to MCAO/IR operations as described in the previous study (Wang et al., 2021). In brief (Diagram 1), The rats (total of 24) used for testing AF toxicity *in vivo* were randomly divided into Sham group (n=12) and Sham+10 mg Albiflorin (AF) group (n=12). Six of the rats in each group were used for neurological scores and pathology examination, and the other six were assessed for detecting brain water content. The rats (total of 54) used for detecting the role and mechanism of AF *in vivo* were randomly divided into Sham group (n=18), MCAO/IR group (n=18), and MCAO/IR+10 mg/kg AF group (n=18). Of the rats in each group, six were used for TTC staining and infarct volume, six for brain water content, and the remaining six for neurological scores, pathological examination, and other tests. We also selected the number of experimental rats by referring to previous studies (Guo et al., 2019; Zhang et al., 2021). AF (C23H28O11) extracted from *Paeonia lactiflora* was purchased from Wuhan ChemFaces Biochemical Co., Ltd (China). Each rat from MCAO/IR group and MCAO/IR+10 mg/kg AF group were anesthetized with isoflurane solution (3% initially and 1-1.5% maintenance) in N_2O and O_2 (3:1) condition and fixed on a plate. The neck was shaved, and a midline incision was performed to separate the fascia, exposing the common carotid artery (CCA), internal carotid artery (ICA), and external carotid artery (ECA). A nylon suture with a heat-passivated end was inserted from CCA into ICA and delivered to the origin of ECA until it blocked the middle cerebral artery (MCA) origin. As a result, blood flow to the right MCA was occluded. After 2h occlusion, the suture was removed carefully from the vessel and reperfused for 24h. AF was dissolved in normal saline. Rats in MCAO/IR group were daily administrated normal saline for 1 week before MCAO/IR. For rats from Sham+10 mg/kg AF group and MCAO/IR+10 mg/kg AF group, an intraperitoneally injection of 10 mg/kg AF was administered daily for 1 week before sham operation or MCAO/IR. The concentration of AF used in rat study was determined according to previous work (Fu et al., 2021; Kim et al., 2021). For rats from Sham group and Sham+10 mg/kg AF group, the right MCA was separated, but no suture was inserted. Then each rat was anesthetized, and brain tissues were immediately removed or restored for further research.

All experimental procedures involved in animals were approved by the Ethics Committee of Pingxiang People's Hospital (Approved number: SYXK (GAN)2019-0007). The work described has been carried out in accordance with the EU Directive 2010/63/EU for animal experiments.

2,3,5-Triphenyltetrazolium chloride (TTC) staining and infarct volume calculation

A neurological score standard was used to assess neurobiological function loss (Longa et al., 1989). The specific criteria are as follows: no deficit (0), failure to extend the right forelimb (1), circling to the opposite side when walking (2), falling to the opposite side while walking (3), and inability to walk spontaneously and loss of consciousness (4). To measure infarct volume, the brain tissues were sliced into 4 coronal sections with a

thickness of 0.2-0.3 cm. Sections were immersed in 2% TTC at 37°C for 30 min. Then the images were scanned and quantified by imaging analysis software (Image J, USA). The infarct volume of the slice was equivalent to the infarct area multiplied by section thickness. The total infarct volume of each brain tissue was calculated by the sum of infarct volumes of all slices. The final infarct volume was corrected by a factor equal to the volume of the non-ischemic/the volume of the ischemic hemisphere to minimize the influence of edema.

Brain water content

Brain water content was detected to assess the cerebral edema condition of rats after cerebral I/R injury. The brain tissues of sacrificed rats were removed immediately. The weights of tissues were measured as wet weight. Then brains were heated for 24h at 105°C in an oven, and the weight of the brain was measured again as dry weight. The value of brain water content is equal to the percentage of wet weight minus dry weight divided by wet weight.

Hematoxylin and eosin (H&E) staining

Brian tissues of rats from different groups were removed after reperfusion for 24h. The tissues were fixed in 10% neutral buffered formalin, embedded in paraffin, and then cut into sections with a thickness of 4 mm. Coronal slices with 5 μm-thickness of the dorsal hippocampus were prepared and stained with H&E.

Statistical analysis

All experiments were at least triplicated. The results of several experiments were shown as mean+standard deviation (SD). Data analyses were carried out by Graphpad 8.0 statistical software (USA). P-values were calculated by One-way ANOVA followed by Dunnett's post hoc test. $P<0.05$ was considered a statistically

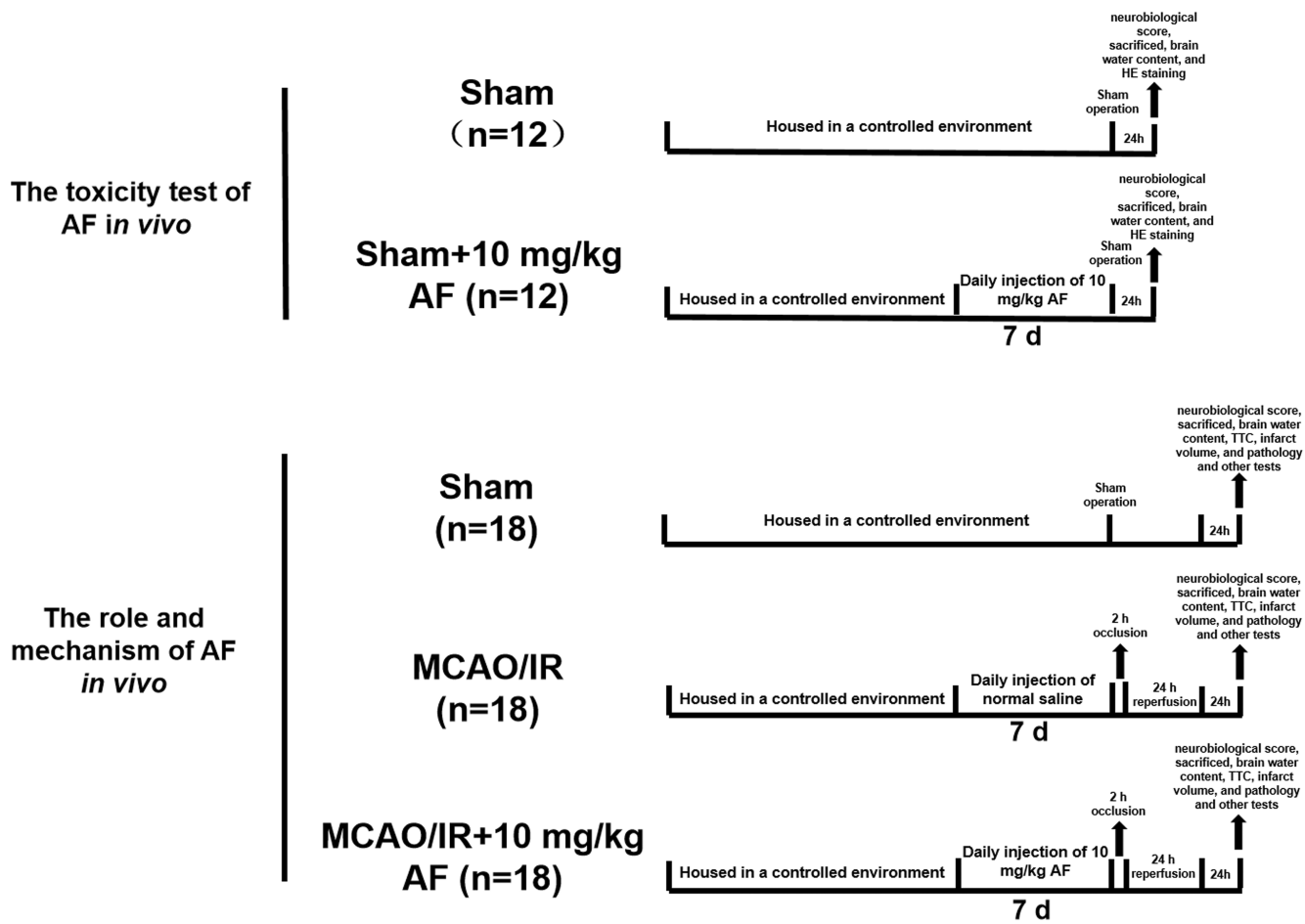

Diagram 1. Flow chart of in vivo experiments.

significant result.

Results

AF promotes cell viability and inhibits apoptosis of OGD/R-stimulated PC-12 cells

The molecular structure of AF was depicted in Fig. 1A. To inquire about the cytotoxicity effect of AF on cell viability, PC12 cells were stimulated with different concentrations of AF, and the viability of cells was monitored by CCK-8 assay. The results displayed that treatment of AF with 1.25-20 μM did not lead to significant cytotoxicity in PC12 cells (Fig. 1B). The effect of AF on OGD/R-treated PC12 cells was explored. OGD/R exposure led to a significant decrease in the viability of PC12 cells, but treatment with AF dose-dependently elevated cell viability (Fig. 1C). Next, we explored the apoptotic effects of AF on PC12 cells triggered by OGD/R. Flow cytometry results showed that OGD/R led to an obvious increase of apoptotic cell rate, however, the use of 5 μM AF dramatically reduced the apoptosis in the cells, and AF treatment with 10 μM and 20 μM had stronger inhibition on apoptosis (Fig. 1D). Similar results were shown in Western blot experiment. The expression levels of pro-apoptotic factors, cleaved caspase-3 and bax, was apparently enhanced, and the expression level of anti-apoptotic protein, bcl-2, was reduced by OGD/R induction in PC12 cells. However, these effects were markedly reversed by AF treatment (Fig. 1E). These results revealed that AF might have protective effects on OGD/R-triggered PC12 cells by promoting viability and inhibiting apoptosis of cells.

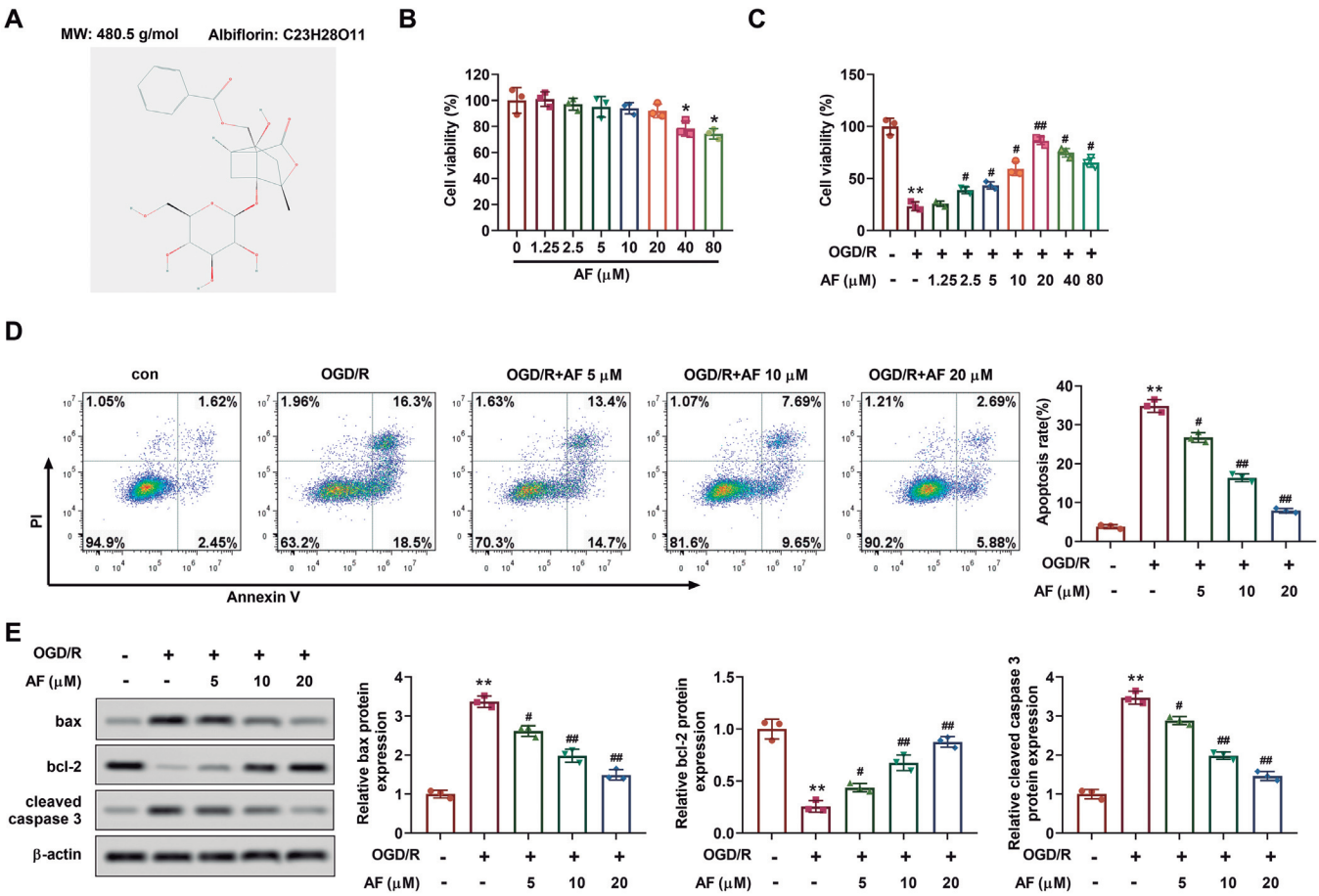

Fig. 1. AF promoted viability and inhibited apoptosis of PC12 cells after OGD/R injury. **A**. The molecular structure of AF was depicted. **B.** CCK-8 assay was used to detect the viability of PC12 cells treated with AF at different concentrations (0, 1.25, 2.5, 5, 10, 20, 40, 80 μM) for 24h. **C.** CCK8 assay was performed to measure the viability of PC12 cells treated with different concentrations of AF (0, 1.25, 2.5, 5, 10, 20, 40, 80 μM) for 24h after OGD/R injury. AF treatment with 20 μM showed the highest ability to restore cell viability, while AF treatment at 40 μM and 80 μM gradually decreased cell viability. **D.** The apoptosis levels of PC12 cells treated with AF at different concentrations (0, 5, 10, 20 μM) for 24h after OGD/R induction were determined by flow cytometry. **E.** Western blot was carried out to assess the protein expression of bax, bcl-2, and cleaved caspase-3 in PC12 cells treated with different concentrations of AF (0, 5, 10, 20 μM) for 24h after OGD/R injury. *p<0.05, **p<0.01 vs. AF (0 μM) group or OGD/R-/AF- group. #p<0.05, ##p<0.01 vs. OGD/R+/AF- group.

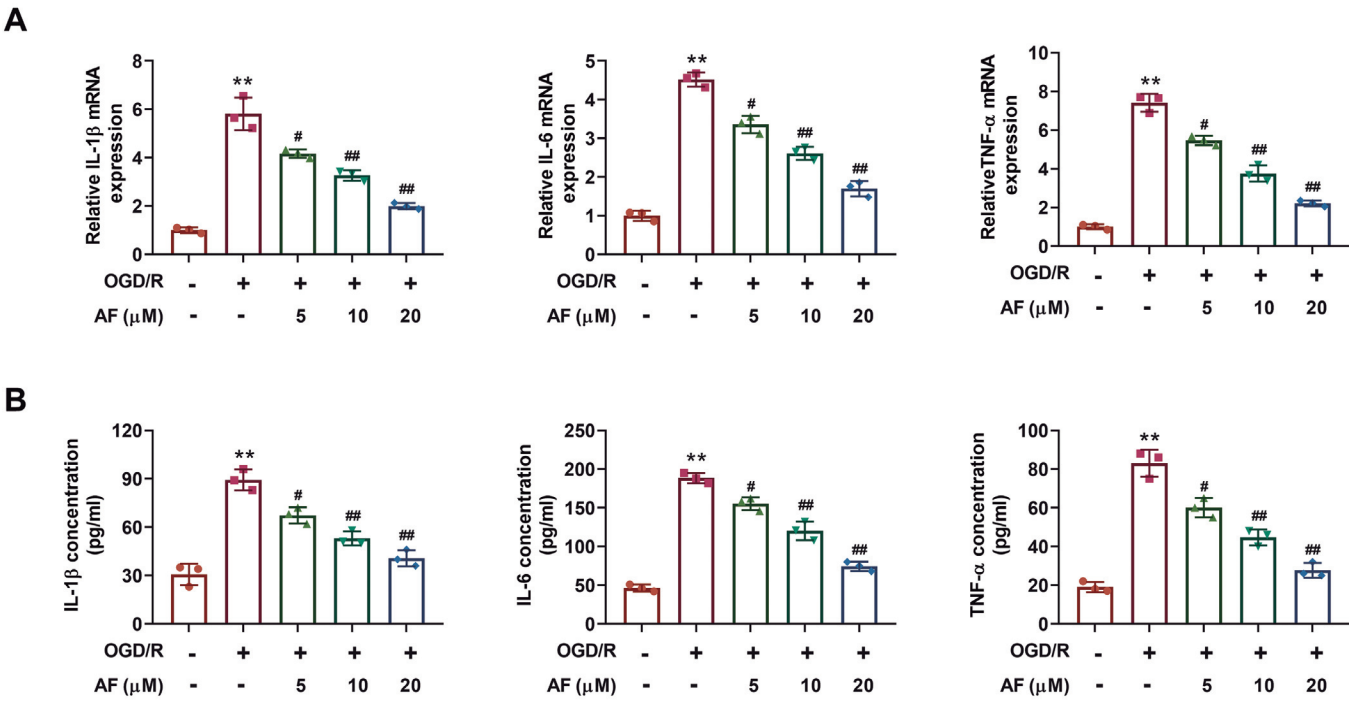

Fig. 2. AF attenuates the inflammatory response induced by OGD/R in PC12 cells. **A.** qRT-PCR was performed to measure mRNA expression levels of IL-1β, IL-6, and TNF-α in PC12 cells treated with AF at different concentrations (0, 5, 10, 20 μM) after OGD/R induction. **B.** ELISA was used to detect the concentrations of IL-1β, IL-6, and TNF-α in PC12 cells treated with AF at different concentrations (0, 5, 10, 20 μM) after OGD/R induction. **p<0.01 vs. OGD/R-/AF- group or control (con) group. #p<0.05, ##p<0.01 vs. OGD/R+/AF- group or OGD/R group.

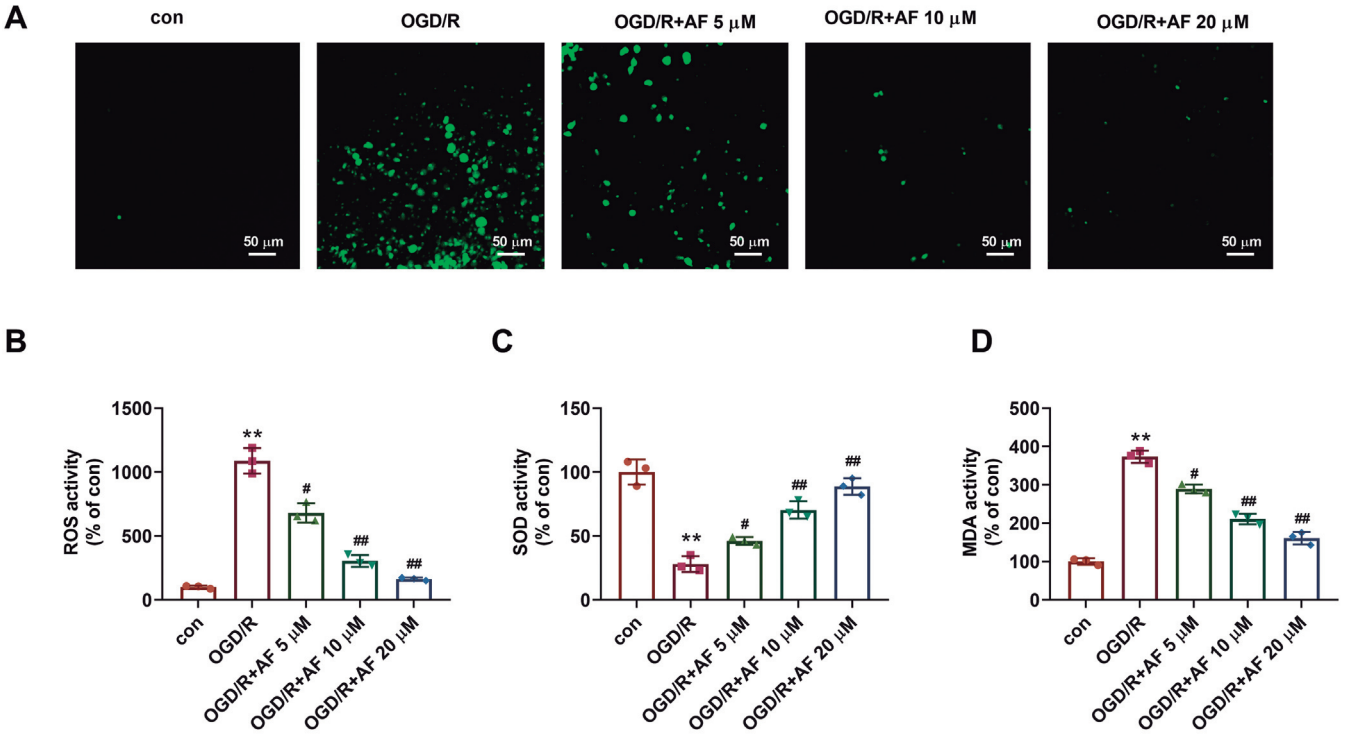

Fig. 3. AF attenuates the oxidative stress induced by OGD/R in PC12 cells. **A.** Immunofluorescence was used to detect the level of ROS in PC12 cells treated with AF at different concentrations (0, 5, 10, 20 μM) after OGD/R induction. **B-D.** The levels of ROS, SOD and MDA in PC12 cells treated with AF at different concentrations (0, 5, 10, 20 μM) after OGD/R induction were detected by the kits. **p<0.01 vs. OGD/R-/AF- group or control (con) group. #p<0.05, ##p<0.01 vs. OGD/R+/AF- group or OGD/R group.

AF attenuates the inflammatory response and oxidative stress triggered by OGD/R in PC12 cells

To further explore the protective effects of AF on OGD/R-triggered PC12 cells, the expression of several inflammatory factors was measured. As depicted in Fig. 2A, the mRNA levels of IL-1β, IL-6, and TNF-α were notably elevated by OGD/R injury in the cells, while treatment with AF reduced the levels of these markers. ELISA also showed that AF treatment effectively ameliorated the concentrations of IL-1β, IL-6, and TNF-α in OGD/R-triggered PC12 cells (Fig. 2B). The DCFH-DA fluorescence intensity was determined by flow cytometry as an indicator of ROS production. A progressive increment of ROS was observed in cells treated with OGD/R, while ROS level was gradually decreased with the increase of AF treatment concentration (Fig. 3A). OGD/R injury significantly decreased the SOD level and enhanced ROS and MDA levels in PC12 cells. However, treatment with AF resulted in a higher level of SOD and a lower level of ROS and MDA compared with the OGD/R group (Fig. 3B-D). Our results suggested that treatment with AF attenuated the inflammatory response and oxidative stress in OGD/R-triggered PC12 cells.

AF alleviates OGD/ R-induced PC12 cell damage by activating Nrf2/HO-1 pathway

To verify the potential mechanism of AF treatment protecting PC12 cells against OGD/R stimulation, changes in Nrf2/HO-1 pathway were examined by Western blot. The OGD/R-induced cells showed obvious elevation in the expression of Nrf2, NQO1, and HO-1. Moreover, the variations of protein expression were significantly enhanced with increased concentrations of AF treatment (Fig. 4A). Next, ML385, an Nrf2 inhibitor, was used to further confirm the activation of Nrf2/HO-1 signaling pathway. Compared with OGD/R+AF (20 μM) group, ML385 caused significant decreases in the expression of Nrf2, NQO1, and HO-1 in OGD/R-stimulated cells (Fig. 4B). The effects on cell viability were presented in Fig. 4C. AF treatment elevated cell viability of OGD/R-triggered cells, while the use of ML385 significantly suppressed the cell viability (Fig. 4C). We also found that the use of ML385 reversed the effects of AF treatment in cell apoptosis (Fig. 4D). Meanwhile, the anti-inflammatory effect of AF in OGD/R-treated cell was ameliorated by ML385 treatment, as indicated by the elevated levels of IL-1β, IL-6, and TNF-α (Fig. 5A). Immunofluorescence

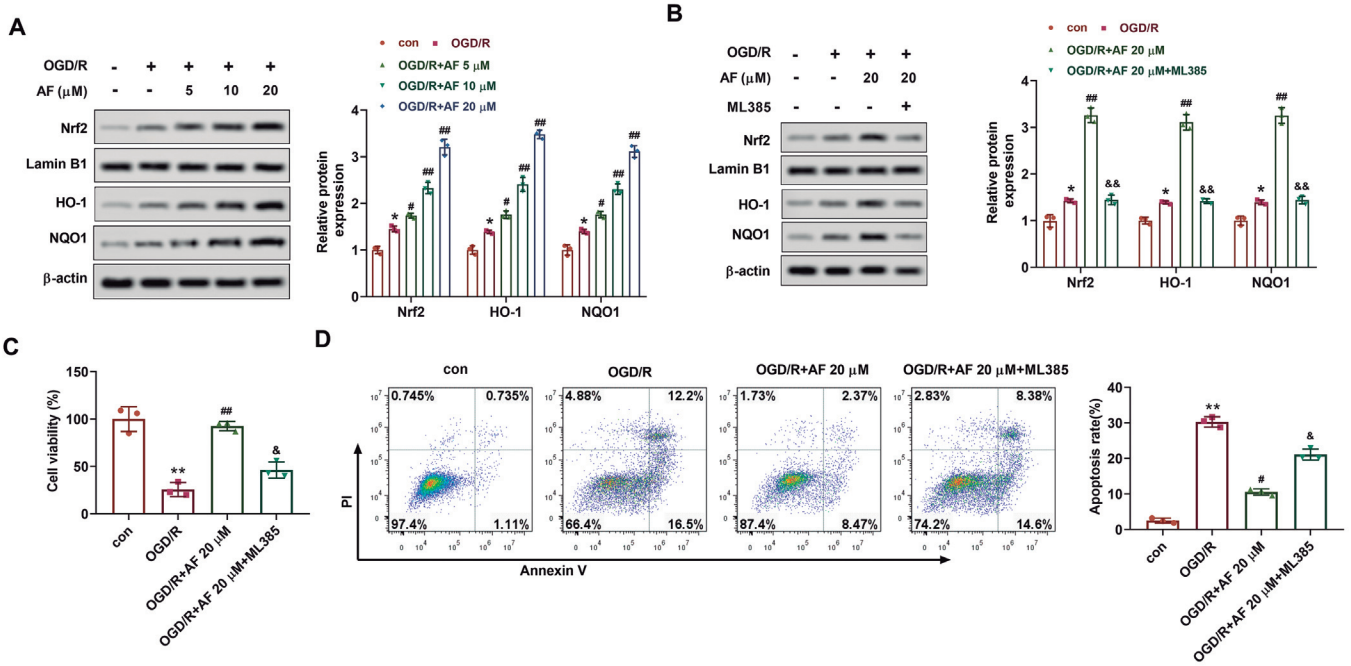

Fig. 4. AF alleviates OGD/ R-induced PC12 cell viability and apoptosis by activating Nrf2/HO-1 pathway. **A.** After OGD/R induction, the levels of nuclear Nrf2 and HO-1, and NQO1 in total proteins in PC12 cells treated with AF at different concentrations (0, 5, 10, 20 μM) were determined by Western blot. **B.** Cells were treated with 5 μM ML385 followed by AF treatment for 24h. The levels of nuclear Nrf2 and NQO1 and HO-1 in total proteins of PC12 cells from different groups (con, OGD/R, OGD/R+AF 20 μM, and OGD/R+AF 20 μM+ML385) were detected by Western blot. **C.** CCK8 assay was used to detect the cell viability of PC12 cells in different groups. **D.** The apoptosis levels of PC12 cells in different groups were detected by flow cytometry. *p<0.05, **p<0.01 vs. OGD/R-/AF- group or control (con) group. #p<0.05, ##p<0.01 vs. OGD/R+/AF- group or OGD/R group. &p<0.05 vs. OGD/R+AF 20 μM group.

showed that ML385 alleviated the inhibiting effect of AF on oxidative stress in the cells, as suggested by the reduced ROS level (Fig. 5B). Our results indicated that AF treatment alleviated OGD/ R-induced PC12 cell damage by activating Nrf2/HO-1 pathway.

AF treatment had no side effects on brain tissues of rats

HE staining was performed to confirm whether AF treatment had damage to rat brain tissues. No abnormal appearance and histological change were observed in the brain tissues of rats from AF treatment group compared with the control group (Fig. 6A). Moreover, there was no apparent difference in neurological deficit score between the sham group and sham+10 mg/kg AF group (Fig. 6B). Consistently, compared with control group, the brain water content of rats showed no significant change after AF treatment (Fig. 6C).

AF reduces cerebral ischemic injury in MCAO/IR rats through activating Nrf2/HO-1 pathway

TTC staining was performed to determine cerebral infarction in MCAO/IR rats treated with AF. The infarcted regions were represented by white-colored areas. There were obvious infarct areas in rat brain tissues from MCAO/IR group, while the infarct areas in 10 mg/kg AF treatment group were remarkably lessened compared with that in MCAO/IR group (Fig. 7A). After MCAO/IR injury, rats displayed apparent neurological deficit, as manifested by the raised neurological score, while AF treatment dramatically decreased neurological deficit score compared with MCAO/IR group (Fig. 7B). The brain water content of rats was markedly lifted by MCAO/IR injury. After AF treatment, the brain water content was significantly lessened compared with that in MCAO/IR group (Fig. 7C). Figure 7D depicted the representative images of HE staining. The sham group showed cells with regular arrangements and well-defined structures. Nevertheless, the MCAO group demonstrated irregular shapes and few inflammatory infiltrations. As anticipated, AF treatment obviously alleviated the damaged and disordered cerebral cells caused by MCAO/IR injury. Furthermore, TUNEL assay revealed that cells in MCAO/IR group were largely apoptotic, while the AF treatment group had a significantly lower

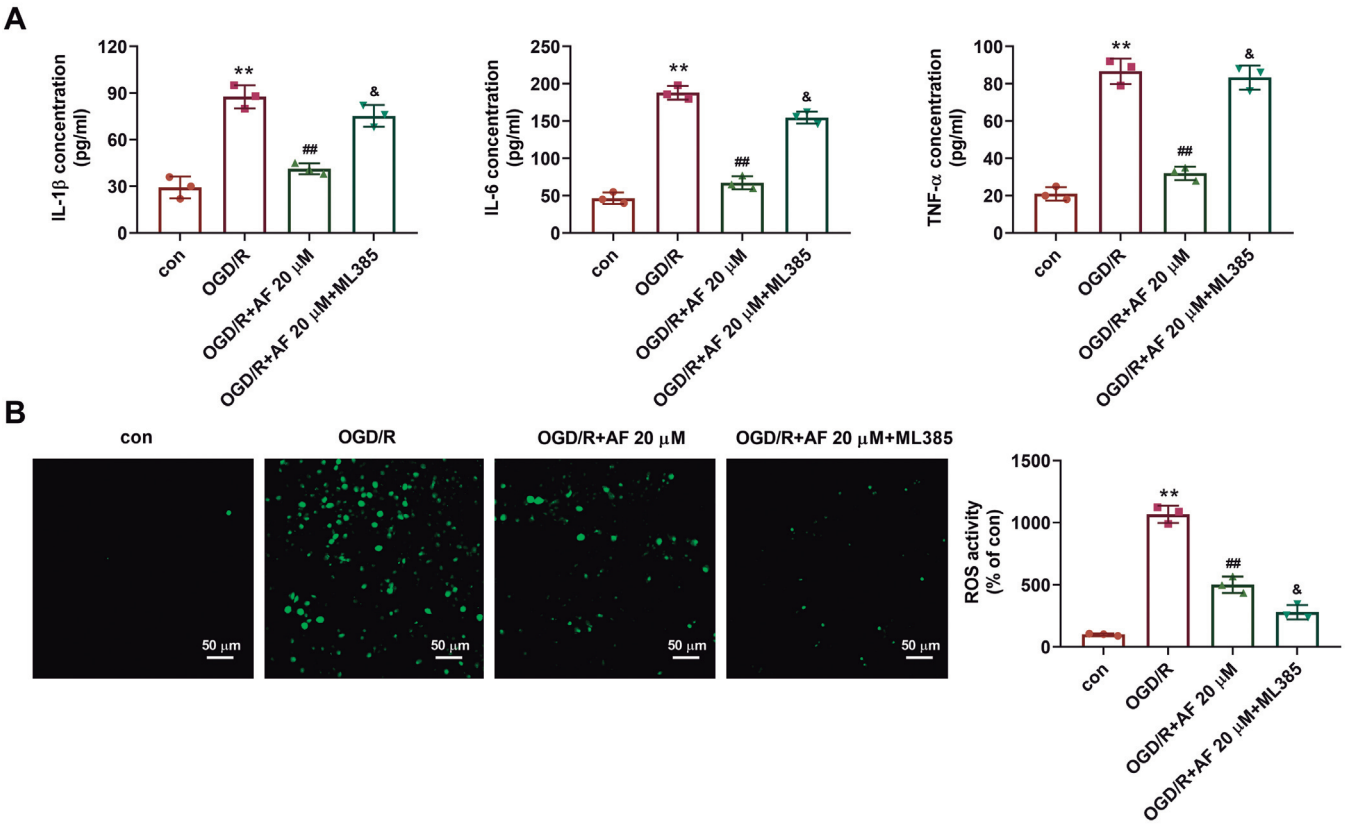

Fig. 5. AF alleviates OGD/ R-induced PC12 cell inflammation and oxidative stress by activating Nrf2/HO-1 pathway. **A.** The levels of IL-1β, IL-6, and TNF-α in different groups of PC12 cells were tested by ELISA. **B.** ROS levels in different groups of PC12 cells were detected by immunofluorescence. *p<0.05, **p<0.01 vs. OGD/R-/AF- group or control (con) group. #p<0.05, ##p<0.01 vs. OGD/R+/AF- group or OGD/R group. &p<0.05 vs. OGD/R+AF 20 μM group.

apoptosis rate (Fig. 7E). As shown in Figure 8A, the inflammatory cytokines, IL-1β, IL-6, and TNF-α, were elevated in brain tissues of rats due to MCAO/IR injury compared with sham group, while AF treatment notably reduced the concentrations of these cytokines. The SOD activity content in MCAO/IR group was markedly lower than that in sham group, and the level of MDA in MCAO/IR group was notably higher than that in sham group. However, treatment with AF showed elevated SOD activity and reduced MDA level compared to the MCAO/IR group (Fig. 8B,C), suggesting that AF mitigated oxidative stress induced by cerebral IR injury. To validate the mechanism of AF protecting brain against MCAO/IR injury, the expression levels of Nrf2, HO-1, and NQO1 proteins were examined by Western blot. The level of nuclear metastasis of Nrf2 and the

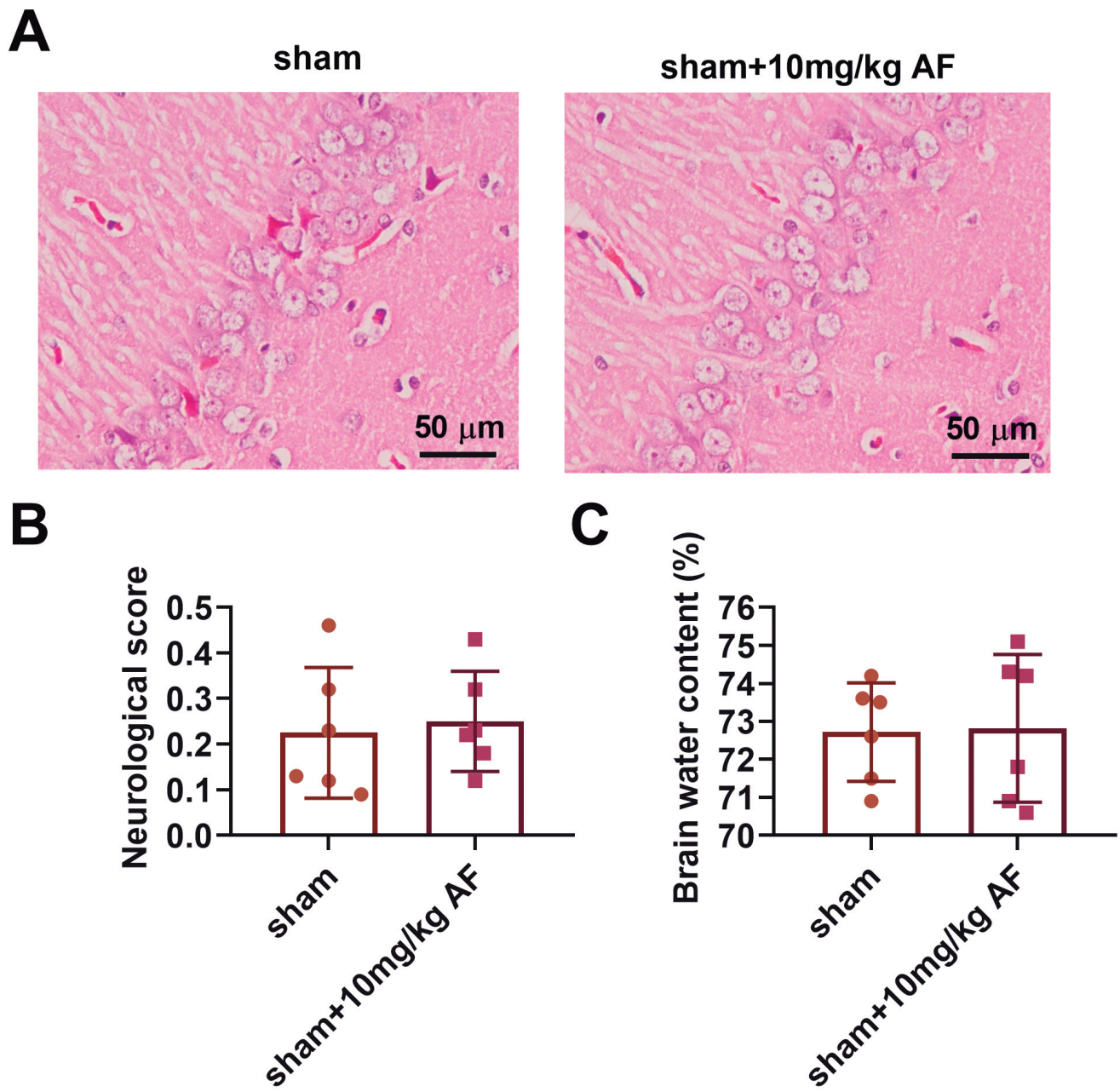

Fig. 6. AF treatment had no side effects on brain tissues of rats. **A.** HE staining was used to detect brain tissue damage in rats from sham operation group (Sham) and AF treatment group (Sham+10 mg/kg AF). **B.** Comparison of neurological deficit score of rats from the two groups. **C.** Comparison of brain water content of rats from the two groups.

protein levels of HO-1 and NQO1 in MCAO/IR group were remarkably higher than those in sham operation group but notably lower than those in 10 mg/kg AF treatment group (Fig. 8D). Our findings indicated that AF exerted a neuroprotective effect in MCAO/IR rats by overexpressing Nrf2/HO-1 pathway.

Discussion

The mortality rate of ischemic cerebrovascular disease is as high as 60%-80%, and the incidence is increasing annually (Dong et al., 2015). The life quality of survivors may also be seriously affected (Zhu et al., 2002). AF is the main monoterpene contained in *P. alba Radix*. The neuroprotective effect of AF has been identified in Parkinson's disease (Ho et al., 2015) and Alzheimer's disease (Zheng et al., 2019). Nevertheless, to our knowledge, there was no research about AF's role and regulatory mechanism in cerebral IR injury. We found that AF treatment had no toxicity to PC12 cells and could improve the cell viability of OGD/R-stimulated PC12 cells.

When cerebral ischemia occurs during reperfusion, compensation provided by nerve cells that already existed in ischemic and hypoxic tissues of brain is suddenly increased, accompanied by a sharp elevation in free radicals that mediate oxidation damage in affected areas (Stegner et al., 2019). MDA, the product of oxidative stress, further aggravates cellular membrane damage. Since SOD serves as the main scavenger of free radicals, the oxidation damage severity in ischemic regions depends on the balance between the levels of SOD and MDA (Naderi et al., 2017). In this process, inflammatory factors, such as IL-1β, TNF-α, and IL-6, might be produced. Except for the increased intracellular inflammatory cell infiltration, these factors also promote extracellular inflammatory mediator release, further aggravating damage in ischemic regions (Yao et al., 2014). Existing reports also showed that oxidants or pro-oxidants are significant regulators of apoptosis (Olanow,

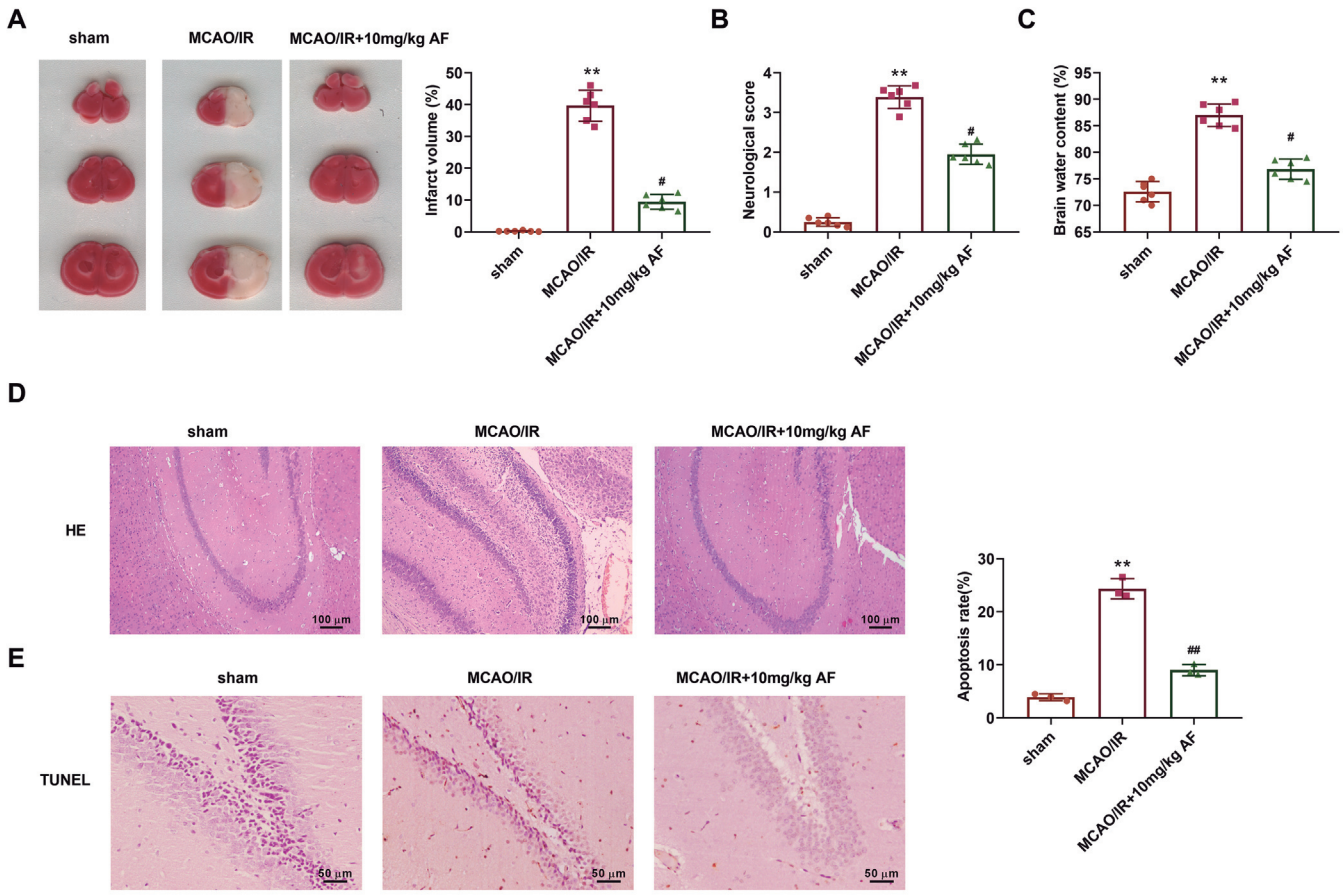

Fig. 7. AF reduces cerebral ischemic injury in MCAO/IR rats. **A.** TTC staining was used to detect cerebral infarction areas in different groups (sham, MCAO/IR, MCAO/IR+10 mg/kg AF) of rats. **B-C.** Effects of AF on neurological deficit score and brain water content were compared among different groups. **D.** HE was performed to determine the pathological damage of brain tissue in different groups of rat models. **E.** TUNEL experiment was performed to detect cell apoptosis in brain tissues from different groups of rat models. The apoptosis rates of cells were quantized with Image J. *p<0.05, **p<0.01 vs. sham group. #p<0.05, ##p<0.01 vs. MCAO/IR group.

1993; Gil et al., 2003). Substances with antioxidant properties can protect against oxidative stress-induced toxic damage and inhibit cell apoptosis by reducing the production of ROS (Gil et al., 2003). Furthermore, the anti-apoptosis, anti-inflammation, and anti-oxidation effects of AF have been documented in various diseases. For instance, AF ameliorated pulmonary inflammation induced by ovalbumin in mice (Cai et al., 2019). AF played anti-apoptosis and anti-oxidative roles in Alzheimer's disease (Xu et al., 2019). Here, in cerebral IR injury models, we found that AF treatment protected neurons against inflammation, oxidation, and apoptosis in vitro and in vivo, which is consistent with previous conclusions.

There is growing evidence that Nrf2 deficiency induces inflammation, apoptosis, and oxidation (Zhang et al., 2017a,b). Nrf2 is a pivotal transcription factor that regulates the anti-oxidant gene in response to oxidation damage (Fu et al., 2021). In this process, activated Nrf2 translocates into nucleus and combines to anti-oxidant response gene promoter region, thereby regulating downstream antioxidant gene expressions, such as HO-1 and NQO1. HO-1 and the enzymatic products have anti-inflammatory, anti-apoptotic, anti-oxidant, and vasodilation actions, and can improve tissue microcirculation (Itoh et al., 1999). It has been reported that Nrf2 could be activated by multiple Chinese herbal medicine formulas or phytochemicals (Li et al., 2020), including AF (Ma et al., 2015). Pelargonidin ameliorates MCAO -induced cerebral/IR injury by the action on the Nrf2/HO-1 pathway in rats (Fu et al., 2021). Research proved that activation of Nrf2 was an underlying therapeutic target for neuroprotection in cerebral IR injury (Zhang et al., 2017a,b). In our study, AF treatment could elevate the expression of Nrf2, HO-1, and NQO1 in vitro and in vivo, which was in line with previous results. Moreover, we used ML385, a widely used Nrf2 inhibitor, to determine the regulation of AF in Nrf2/HO-1 pathway. Preserving and maintaining the activity of the Nrf-2 pathway can counteract oxidative stress and subsequent inflammation following ischemic and traumatic brain injury (Dong et al., 2015). Nrf2 inhibition abolished the protective function of AF on cell viability, apoptosis, inflammation, and oxidative stress, indicating that AF conferred its protective effects against cerebral IR injury via activating Nrf2/HO-1 pathway.

In the current study, MCAO method was used to construct the cerebral IR model in rats. MCAO/IR is classical and frequently used in vivo model for ischemic cerebrovascular disease because of its patho-

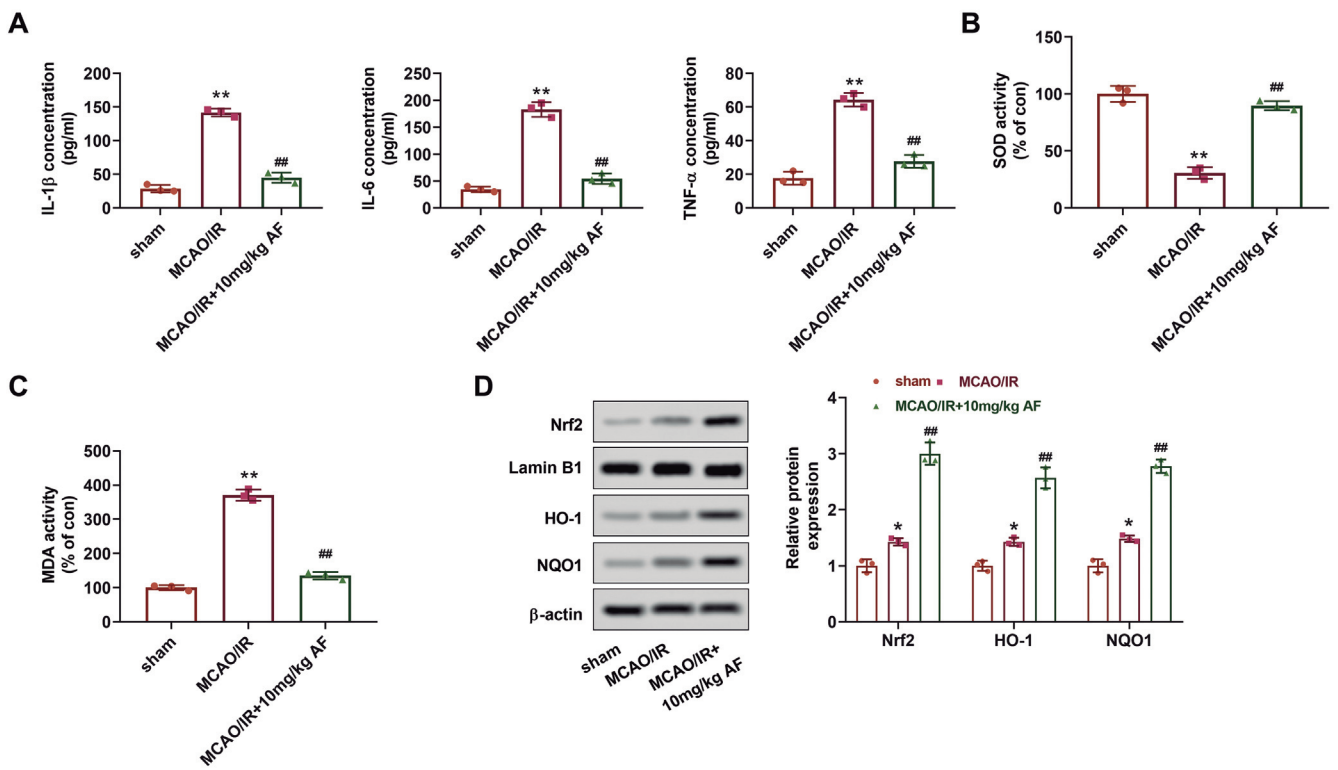

Fig. 8. AF reduces cerebral ischemic injury in MCAO/IR rats through activating Nrf2/HO-1 pathway. **A.** ELISA was used to measure the levels of IL-1β, IL-6, and TNF-α in the hippocampus of rat brain tissues from different groups. **B-C.** The concentrations of SOD and MDA in rat brain tissues from different groups were determined by the kits. **D.** The levels of nuclear Nrf2 and NQO1 and HO-1 in total proteins of rat brain tissues from different groups were detected by Western blot. *p<0.05, **p<0.01 vs. sham group. #p<0.05, ##p<0.01 vs. MCAO/IR group.

physiological and gene expression level changes similar to those in human body (Fusco et al., 2019). The results of this work showed significant neurological deficits in rats 24h after reperfusion. Inflammation is the most crucial degenerative factor after ischemia, which results in sustained brain injury and cerebral edema. TTC results showed that the right frontal lobe, parietal lobe, and caudate nucleus in MCAO/IR group had pale infarcts with clear boundaries, and the quantitative results displayed that the cerebral infarction volume and water contents in brain tissues increased dramatically. The anti-apoptotic, anti-oxidation, and anti-inflammatory effects of AF on neuroprotection have been described in other animal models. In Alzheimer's mouse model, AF exerts an anti-oxidant effect by reducing ROS level and increasing SOD activity, and reduces the number of apoptotic cells in the anterior parietal cortex of mice by increasing the level of bcl-2 and decreasing the levels of bax and caspase-3 in hippocampus and cortex (Xu et al., 2019). In a mouse model of Parkinson's disease, a prescription of traditional Chinese medicine containing AF was able to block apoptosis (Zhang et al., 2017c). AF could significantly decrease the levels of TNF-α, IL-1β, and IL-6 in the serum and hippocampus of Alzheimer's rat models induced by streptozotocin (Wu et al., 2019). Our study indicated that AF could effectively attenuate neurological deficits, cerebral infarct volume, and brain water contents in MCAO/IR rats. Further, AF could ameliorate apoptosis, inflammatory response, and oxidative stress that occurred in MCAO/IR-induced rat models, which was in line with previous conclusions, and the application of AF could promote the neuroprotective effect in vivo via activating Nrf2/HO-1 pathway.

Conclusions

The present work demonstrated that AF alleviated cerebral IR injury by enhancing neuronal cell viability in vitro and attenuating apoptosis, inflammation, and oxidation *in vitro* and *in vivo*. Moreover, our experiments identified that the neuroprotective effects of AF in cerebral IR were achieved by activating Nrf2/HO-1 pathway. Our findings provided novel insights into developing agents for cerebral IR injury and protecting against cerebral ischemia.

Acknowledgements. None.

Conflict of interest. The authors state no conflict of interest.

Data availability statement. The datasets used and/or analyzed during the current study are available from the corresponding author on reasonable request.

Funding. None.

Author contribution. RunYing Li contributed to conception and design. Fei Zhu and Jianzhong Xiong performed animal and cell experiments. Fei Yi, Ermin Luo, and Chun Huang analyzed the experimental data. Fei Zhu wrote the initial draft. All authors have read and approved the manuscript.

References

Block L., El-Merhi A., Liljencrantz J., Naredi S., Staron M. and Odenstedt Hergès H. (2020). Cerebral ischemia detection using artificial intelligence (CIDAI)-a study protocol. Acta Anaesthesiol. Scand. 64, 1335-1342.

Bramlett H.M. and Dietrich W.D. (2004). Pathophysiology of cerebral ischemia and brain trauma: Similarities and differences. J. Cereb. Blood Flow Metab. 24, 133-150.

Cai Y., Yang E., Yao X., Zhang X., Wang Q., Wang Y., Liu J., Fan W., Yi K., Kang C. and Wu J. (2021). FUNDC1-dependent mitophagy induced by tPA protects neurons against cerebral ischemia-reperfusion injury. Redox Biol. 38, 101792.

Cai Z., Liu J., Bian H. and Cai J. (2019). Albiflorin alleviates ovalbumin (OVA)-induced pulmonary inflammation in asthmatic mice. Am. J. Transl. Res. 11, 7300-7309.

Dong L., Hou R., Xu Y., Yuan J., Li L., Zheng C. and Zhao H. (2015). Analyzing the correlation between the level of serum markers and ischemic cerebral vascular disease by multiple parameters. Comput. Math. Methods Med. 2015, 972851.

Fu K., Chen M., Zheng H., Li C., Yang F. and Niu Q. (2021). Pelargonidin ameliorates MCAO-induced cerebral ischemia/reperfusion injury in rats by the action on the Nrf2/HO-1 pathway. Transl. Neurosci. 12, 020-031.

Fusco R., Scuto M., Cordaro M., D'Amico R., Gugliandolo E., Siracusa R., Peritore A.F., Crupi R., Impellizzeri D., Cuzzocrea S. and Di Paola R. (2019). N-palmitoylethanolamide-oxazoline protects against middle cerebral artery occlusion injury in diabetic rats by regulating the SIRT1 pathway. Int. J. Mol. Sci. 20, 4845.

Gil J., Almeida S., Oliveira C.R. and Rego A.C. (2003). Cytosolic and mitochondrial ROS in staurosporine-induced retinal cell apoptosis. Free Radic. Bio. Med. 35, 1500-1514.

Ginet V., Puyal J., Clarke P.G.H. and Truttmann A.C. (2009). Enhancement of autophagic flux after neonatal cerebral hypoxia-ischemia and its region-specific relationship to apoptotic mechanisms. Am. J. Pathol. 175, 1962-1974.

Guo P., Jin Z., Wu H., Li X., Ke J., Zhang Z. and Zhao Q. (2019). Effects of irisin on the dysfunction of blood-brain barrier in rats after focal cerebral ischemia/reperfusion. Brain Behav. 9, 1-9.

Ho S.-L., Poon C.-Y., Lin C., Yan T., Kwong D.W.-J., Yung K.K.-L., Wong M.S., Bian Z. and Li H.-W. (2015). Inhibition of β-amyloid aggregation by albiflorin, aloeemodin and neohesperidin and their neuroprotective effect on primary hippocampal cells against β-amyloid induced toxicity. Curr. Alzheimer Res. 12, 424-433.

Ikeda Y., Tajima S., Izawa-Ishizawa Y., Kihira Y., Ishizawa K., Yoshida S., Aihara K.-i., Tsuchiya K. and Tamaki T. (2013). Bovine milk-derived lactoferrin exerts proangiogenic effects in an Src-Akt-eNOS-dependent manner in response to ischemia. J. Cardiovasc. Pharmacol. 61, 423-429.

Itoh K., Wakabayashi N., Katoh Y., Ishii T., Igarashi K., Engel J.D. and Yamamoto M. (1999). Keap1 represses nuclear activation of antioxidant responsive elements by Nrf2 through binding to the amino-terminal Neh2 domain. Genes Dev. 13, 76-86.

Kim J.H., Kim M., Hong S.Y., Kim E.Y., Lee H., Jung H.S. and Sohn Y. (2021). Albiflorin promotes osteoblast differentiation and healing of rat femoral fractures through enhancing BMP-2/Smad and Wnt/β-Catenin signaling. Front. Pharmacol. 12, 1-19.

Li B., Nasser M.I., Masood M., Adlat S., Huang Y., Yang B., Luo C. and Jiang N. (2020). Efficiency of traditional chinese medicine targeting

the Nrf2/HO-1 signaling pathway. Biomed. Pharmacother. 126, 110074.

Longa E.Z., Weinstein P.R., Carlson S. and Cummins R. (1989). Reversible middle cerebral artery occlusion without craniectomy in rats. Stroke 20, 84-91.

Ma X., Zhao Y.-l., Zhu Y., Chen Z., Wang J.-b., Li R.-y., Chen C., Wei S.-z., Li J.-y., Liu B., Wang R.-l., Li Y.-g., Wang L.-f. and Xiao X.-h. (2015). *Paeonia lactiflora* pall. Protects against anit-induced cholestasis by activating Nrf2 via PI3K/Akt signaling pathway. Drug. Des. Devel. Ther. 9, 5061-5074.

Naderi Y., Sabetkasaei M., Parvardeh S. and Zanjani T.M. (2017). Neuroprotective effect of minocycline on cognitive impairments induced by transient cerebral ischemia/reperfusion through its anti-inflammatory and anti-oxidant properties in male rat. Brain Res. Bull. 131, 207-213.

Naderi Y., Panahi Y., Barreto G.E. and Sahebkar A. (2020). Neuroprotective effects of minocycline on focal cerebral ischemia injury: A systematic review. Neural. Regen. Res. 15, 773-782.

Olanow C.W. (1993). A radical hypothesis for neurodegeneration. Trends Neurosci. 16, 439-444.

Song J., Hou X., Hu X., Lu C., Liu C., Wang J., Liu W., Teng L. and Wang D. (2015). Not only serotonergic system, but also dopaminergic system involved in albiflorin against chronic unpredictable mild stress-induced depression-like behavior in rats. Chem. Biol. Interact. 242, 211-217.

Stegner D., Klaus V. and Nieswandt B. (2019). Platelets as modulators of cerebral ischemia/reperfusion injury. Front. Immunol. 10, 2505.

Wang B., Cao W., Biswal S. and Doré S. (2011). Carbon monoxide-activated Nrf2 pathway leads to protection against permanent focal cerebral ischemia. Stroke 42, 2605-2610.

Wang L., Tan Y., Zhu Z., Chen J., Sun Q., Ai Z., Ai C., Xing Y., He G. and Liu Y. (2021). ATP2B1-AS1 promotes cerebral ischemia/reperfusion injury through regulating the miR-330-5p/TLR4-MyD88-NF-κB signaling pathway. Front. Cell Dev. Biol. 9.

Wu T., Yin F., Kong H. and Peng J. (2019). Germacrone attenuates cerebral ischemia/reperfusion injury in rats via antioxidative and antiapoptotic mechanisms. J. Cell Biochem. 120, 18901-18909.

Wu L., Xiong X., Wu X., Ye Y., Jian Z., Zhi Z. and Gu L. (2020). Targeting oxidative stress and inflammation to prevent ischemia-reperfusion injury. Front. Mol. Neurosci. 13, 1-13.

Xu Y.-J., Mei Y., Shi X.-Q., Zhang Y.-F., Wang X.-Y., Guan L., Wang Q. and Pan H.-F. (2019). Albiflorin ameliorates memory deficits in APP/PS1 transgenic mice via ameliorating mitochondrial dysfunction. Brain Res. 1719, 113-123.

Yao Y., Chen L., Xiao J., Wang C., Jiang W., Zhang R. and Hao J. (2014). Chrysin protects against focal cerebral ischemia/reperfusion injury in mice through attenuation of oxidative stress and inflammation. Int. J. Mol. Sci. 15, 20913-20926.

Zhang R., Xu M., Wang Y., Xie F., Zhang G. and Qin X. (2017a). Nrf2-a promising therapeutic target for defensing against oxidative stress in stroke. Mol. Neurobiol. 54, 6006-6017.

Zhang W., Wei R., Zhang L., Tan Y. and Qian C. (2017b). Sirtuin 6 protects the brain from cerebral ischemia/reperfusion injury through Nrf2 activation. Neuroscience 366, 95-104.

Zhang J., Zhang Z., Bao J., Yu Z., Cai M., Li X., Wu T., Xiang J. and Cai D. (2017c). Jia-jian-di-huang-yin-zi decoction reduces apoptosis induced by both mitochondrial and endoplasmic reticulum caspase12 pathways in the mouse model of parkinson's disease. J. Ethnopharmacol. 203, 69-79.

Zhang Z.N., Hui Z., Chen C., Liang Y., Tang L.L., Wang S.L., Xu C.C., Yang H., Zhang J.S. and Zhao Y. (2021). Neuroprotective effects and related mechanisms of echinacoside in MPTP-induced PD mice. Neuropsychiatr. Dis. Treat. 17, 1779-1792.

Zheng M., Liu C., Fan Y., Shi D. and Jian W. (2019). Total glucosides of paeony (TGP) extracted from *radix Paeoniae alba* exerts neuroprotective effects in MPTP-induced experimental parkinsonism by regulating the cAMP/PKA/CREB signaling pathway. J. Ethnopharmacol. 245, 112182.

Zhou J., Wang L., Wang J., Wang C., Yang Z., Wang C., Zhu Y. and Zhang J. (2016). Paeoniflorin and albiflorin attenuate neuropathic pain via MAPK pathway in chronic constriction injury rats. Evid. Based Complement. Alternat. Med. 2016, 8082753.

Zhu M., Dai J. and Li S. (2002). Cerebral angiography and MR perfusion images in patients with ischemic cerebral vascular disease. Chin. Med. J. (Engl). 115, 1687-1691.

Zhu X., Jing L., Chen C., Shao M., Fan Q., Diao J., Liu Y., Lv Z. and Sun X. (2015). Danzhi xiaoyao san ameliorates depressive-like behavior by shifting toward serotonin via the downregulation of hippocampal indoleamine 2,3-dioxygenase. J. Ethnopharmacol. 160, 86-93.

Accepted September 19, 2022